Asian Journal of Chemistry; Vol. 37, No. 10 (2025), 2525-2531
ASIAN JOURNAL OF CHEMISTRY
https://doi.org/10.14233/ajchem.2025.34478

Therapeutic Evaluation of *Zanthoxylum armatum* Leaves Extract and its Green Synthesized Silver Nanoparticles for Antidiabetic and Cytotoxic Applications

MOHIT KUMAR, SWATI JAAST and ANIL KUMAR*

Department of Biotechnology, Guru Jambheshwar University of Science and Technology, Hisar-125001, India

*Corresponding author: E-mail: bhankhar@gmail.com

Received: 18 July 2025 *Accepted*: 19 September 2025 *Published online*: 30 September 2025 AJC-22137

Targeting digestive enzymes presents a promising strategy for preventing, treating and managing diabetes. The present study evaluated the cytotoxic and antidiabetic potential of the leaves extract of *Zanthoxylum armatum* (ZAE) and silver nanoparticles (ZA-Ag NPs) using an *in vitro* approach. The Ag NPs were synthesized biologically and characterized using advanced analytical instruments, including UV-Vis spectrophotometry, dynamic light scattering (DLS), Fourier transform infrared spectroscopy (FTIR), field-emission scanning electron microscopy (FE-SEM) and X-ray diffraction (XRD). Enzyme inhibition assays were performed against α-amylase, α-glucosidase, β-glucosidase and lipase. The cytotoxicity of silver nanoparticles was also evaluated. UV-visible spectroscopy showed a peak at 429 nm. DLS analysis indicated that Ag NPs have a Z-average size of 92 nm along with zeta potentials of -13.2. FE-SEM revealed that the nanoparticles were spherical, with some dispersed and others present as agglomerates. FTIR analysis identified the functional groups of Ag NPs and the XRD spectrum confirmed their crystalline nature. Their antidiabetic properties increased in a concentration-dependent manner. *Z. armatum* derived silver nanoparticles (ZA-Ag NPs) exhibited IC_{50} values of 81.82, 75.72, 111.71 and 59.02 µg/mL, whereas *Z. armatum* extract (ZAE) showed 77.52, 82.77, 120.08 and 49.24 µg/mL against α-amylase, α-glucosidase, β-glucosidase and lipase respectively. ZA-Ag NPs demonstrated stronger inhibition of α-amylase, α-glucosidase and β-glucosidase, while ZAE was more effective against lipase. The results were further validated by one-way ANOVA, confirming significant enzyme inhibition by Ag NPs ($p < 0.05$).

Keywords: Nanoparticles, Antidiabetic, Cytotoxicity, *Zanthoxylum armatum*, Biogenic.

INTRODUCTION

Approximately 80% of the global diabetes burden is concentrated in low and middle income countries, with middle income nations alone accounting for 78% [1,2]. According to the 11th edition of the International Diabetes Federation (IDF) 2025, diabetes is one of the fastest-growing health challenges of the 21st century. In 2024, an estimated 589 million adults aged 20 to 79 were living with diabetes, including over 9.5 million diagnosed with type 1 diabetes, 1.9 million of whom were children and adolescents under 20. By 2050, the global number is expected to rise to 853 million. India has the second highest number of diabetes cases after China. Over the past three decades, prevalence in India has surged from 65 million in 2016 to 77 million in 2019 and 89.8 million in 2024. Projections indicate this could rise to 156.7 million by 2050, highlighting the increasing burden of the disease [3].

Medicinal plants contain bioactive compounds [4,5] that help regulate blood glucose by enhancing insulin activity and protecting pancreatic cells. Nanotechnology improves the delivery and effectiveness of these plant-based compounds, offering a green, targeted and efficient approach. Together, they provide a promising strategy for safer and more effective diabetes treatment [6]. Rich in both primary and secondary metabolites, such as proteins, vitamins, carbohydrates, terpenes, flavonoids, alkaloids, phenolics, lipids, saponins and tannins, they not only serve as valuable herbal medicines but also act as natural reducing and capping agents in the green synthesis of nanoparticles [7,8]. Furthermore, phytochemicals, with their intrinsic biological activity, can enhance the therapeutic efficacy of nanoparticles by improving targeted delivery and minimizing off-target toxicity [9,10]. When conjugated with nanoparticles, these bioactive plant-derived compounds can synergistically induce apoptosis in cancer cells through oxidative stress pathways, mito-chondrial dysfunction and cell cycle arrest. Moreover, the biocompatibility and eco-friendly nature of plant-mediated nanoparticles make them promising candidates for anticancer drug delivery systems. Thus, integ-

rating phytochemicals with nanotechnology offers a novel and effective strategy for cancer therapy, combining the cytotoxic potency of natural compounds with the precision of nanoscale drug delivery [11].

One such plant, *Zanthoxylum armatum*, a member of the Rutaceae family, thrives across the subtropical Himalayas (ranging from Kumaon to Khasi Hills). It is widely distributed across Eastern and Southeast Asia, including countries such as India, Nepal, Bhutan, China, Pakistan, Taiwan, Malaysia, Japan, and the Philippines [12]. It is famous as Indian prickly ash, Nepali Dhania and timur and is extensively used in Indian medicines [13-15]. This plant is widely used in traditional medicine for treating various ailments, including diabetes, respiratory diseases, cancer, metabolic disorders, toothaches, headaches and diarrhoea [16]. The leaves are known for their anti-inflammatory, antioxidant and antihelmintic properties [17]. The evidence suggests that aqueous extracts of *Z. armatum* leaves exhibit anti-diabetic properties in mice models [18,19]. Moreover, the methanolic extracts of the stem bark were found to exhibit antiproliferative activity, inhibiting the growth of human keratinocytes [20]. Despite this potential, there is limited research on the antidiabetic and cytotoxic effects of *Z. armatum* leaves extract and its biosynthesized Ag NPs. This study aims to evaluate the antidiabetic and cytotoxic potentials of both the plant extract and the Ag NPs synthesized from it.

EXPERIMENTAL

In this work, the chemical, reagents and enzymes *viz*., dimethyl sulfoxide, isopropanol, 3-(4,5-dimethylthiazol-2-yl)-2,5-diphenyltetrazolium bromide, phosphate buffer, silver nitrate, sodium phosphate (both monobasic as well dibasic), α-amylase, α-glucosidase, β-glucosidase, lipase, acarbose and orlistat were purchased from SRL, Sigma and Himedia, India. All chemicals were of analytical grade and used as such. While the solutions were freshly prepared in double-distilled water and autoclaved as required.

Collection of plant samples: The fresh leaves of *Z. armatum* were collected from wild population of Ramban forest of Jammu and Kashmir area, India. The samples were authenticated, cleaned and shade dried for one week before extraction.

Preparation of plant extract: The aqueous leaves extract of *Z. armatum* was prepared as described earlier [21]. The dried leaves were grinded to fine powder and 10 g of this powder was mixed with 100 mL of distilled water and incubated at 40 ºC with shaking at 150 rpm for 5-7 days. The filtrate was evaporated in a fume hood and the residue was dissolved in DMSO for further studies.

Biogenic synthesis of silver nanoparticles: The silver nanoparticles were synthesized using the method proposed by Bhardwaj & Gupta [22] with minor modifications. The silver nanoparticles were prepared by mixing of 20 mL of ZAE with 80 mL of 1 mM $AgNO_3$ in a conical flask. The resultant solution was then kept on the magnetic stirrer at 71 ºC until a visible colour change indicated the formation of silver nanoparticles.

Characterization: UV-Vis spectroscopy was employed to confirm the synthesis of Ag NPs using UV-Vis spectrophotometer (Varian Inc., USA) from 300 to 600 nm [23]. DLS analysis was performed using a Zetasizer (Malvern Instruments, UK), to determine the polydispersity index (PDI) and hydrodynamic diameter of the nanoparticles [24]. The morphological features and functional groups of synthesized Ag NPs were examined by SEM (SEM, JSM-7610FPlus, JEOL) and FTIR (Spectrum Two/Perkin Elmer) [25]. X-ray diffraction studies were performed using XRD (SmartLab 3KW/Rigaku) to determine the crystallinity of the biosynthesized Ag NPs [26].

Cytotoxic activity: The cytotoxicity of the leaves extract of *Z. armatum* (ZAE) and silver nanoparticles (ZA-Ag NPs) was assessed using the MTT assay described by Njeru & Muema [27], on Vero cells derived from African green monkey kidney cells (ATCC CCL-81). Cells were seeded in 96-well plates and exposed to varying concentrations of the extract and Ag NPs (ranging from 50-0.02 μg/mL) under standard culture conditions (37 ºC, 5% CO_2) at 1.0×10^5 cells/mL. After 48 h of incubation, 10 μL of MTT solution (5 mg/mL) was added to each well and incubated for an additional 4 h. Subsequently, 100 μL of acidified isopropanol (0.04 N HCl) was added. The plates were shaken gently to dissolve the formazan and the absorbance was measured at 562 nm with a reference wavelength of 690 nm using an ELISA plate reader (Lab Systems–Multiskan EX). Medium without sample is used as a control and with 1% DMSO as a negative control. Cell viability (%) was calculated using the following formula [28]:

$$\text{Cell viability (\%)} = \frac{\text{OD of sample at } 562 - \text{OD690}}{\text{OD of control } 562 - \text{OD690}} \times 100$$

Antidiabetic activity

α-Amylase inhibition assay: The α-amylase assay was adapted from the reported method [29], with slight modifications. Silver nanoparticles and crude extract were prepared at various concentrations (20, 40, 60, 80 and 100 μg/mL) in 0.02 M sodium phosphate buffer (pH 6.9). To each sample tube, 200 μL of α-amylase (porcine pancreatic) solution (10 U/mL) was added and incubated for 15 min at 35 ºC. Following this, 200 μL of 1% starch solution was added and the mixture was incubated at 35 ºC for 10 min. The reaction was halted by adding the DNS reagent, followed by heating the mixture at 85 ºC for 15 min. After cooling to room temperature, the absorbance was measured at 540 nm.

α-Glucosidase inhibition assay: The α-glucosidase inhibitory activity of the plant extract (ZAE) and ZAE based Ag nanoparticles (ZA-Ag NPs) was evaluated following the method described earlier [30], with slight modifications. Briefly, 500 μL of plant extract or nanoparticles (at concentrations ranging from 20 to 100 μg/mL) was mixed with 100 μL of α-glucosidase enzyme (from yeast, 1 U/mL) in 0.1 M phosphate buffer (pH 6.8) and incubated at 37 ºC for 15 min. After incubation, 200 μL of 1 M *p*-nitrophenyl-α-D-glucopyranoside (α-pNPG) substrate was added, and the mixture was further incubated at room temperature for 20 min. The reaction was stopped with 0.1 M sodium carbonate (500 μL) and the absorbance was recorded at 405 nm.

β-Glucosidase inhibition assay: The inhibition of β-glucosidase with ZA-Ag NPs and plant extracts was carried out according to [31]. In a 96-well plate, the reaction mixture

containing 20 µL *p*-nitrophenyl-β-D-glucopyranoside (β-pNPG), 10 µL of sample (20-100 µg/mL) and 20 µL of sodium phosphate buffer (pH 5) was incubated for 10 min at 37 ºC. Then, 10 µL of β-glucosidase (sweet almond) was added, followed by 30 min incubation at 37 ºC. The reaction was stopped with 140 µL of sodium phosphate buffer (pH 10) and the absorbance was measured at 410 nm.

Lipase inhibition assay: The *in vitro* lipase inhibition assay was performed according to the reported method [32], with some modifications. ZAE, ZA-Ag NPs and orlistat (1 mg/mL in 10% DMSO) at varying concentrations (20-100 µg/mL) were mixed with 100 µL of lipase solution (1 mg/mL) and adjusted to 1 mL with Tri-HCl buffer (pH 7.4), followed by incubation at 25 ºC for 15 min. Subsequently, 100 µL of substrate *p*-nitrophenyl butyrate (pNPB) (20.9 mg dissolved in 2 mL of acetonitrile) was added to the mixture. It was then incubated for another 30 min at 37 ºC and the absorbance was recorded at 405 nm. The inhibition percentage of all antidiabetic assays was calculated using the formula:

$$\text{Inhibition } (\%) = \frac{\text{Abs of control} - \text{Abs of sample}}{\text{Abs of control}} \times 100$$

Acarbose was used as a positive control for α-amylase, α-glucosidase and β-glucosidase inhibition assays, whereas orlistat was used for lipase inhibition**.** The results were expressed as IC_{50} values, presenting the amount of extracts and nanoparticles required to achieve 50% enzyme inhibition.

Statistical analysis: All experiments were performed in triplicates and analyzed statistically using One-Way ANOVA ($p < 0.05$) with the SPSS program. IC_{50} was determined by regression analysis using Microsoft Excel.

RESULTS AND DISCUSSION

The addition of crude plant extract to the silver nitrate solution resulted in the distinct physico-chemical changes. The colour change of the reaction mixture from light green to dark brown, considered an initial indicator of Ag NPs formation, suggests that bioactive compounds play a crucial role in the synthesis of silver nanoparticles [33]. The dark brown colour of the reaction mixture, initially confirms the formation of Ag NPs. These results align with previous reports on colour changes in plant-based synthesis of Ag NPs [34].

UV-visible studies: The UV-Vis spectrum displayed a distinct and strong absorption peak at 429 nm (Fig. 1a), confirming the formation of Ag NPs. This observation aligns with earlier studies, which have shown that silver nanoparticles typically exhibit a strong surface plasmon resonance (SPR) absorption band within the range of 410-455 nm [25]. Similarly, Quadri *et al.* [26] observed a peak at 430 nm for Ag NPs synthesized using the fruit extract of *Z. armatum*.

FT IR studies: The FTIR analysis of both leaves extract and Ag NPs was performed to identify the potential functional groups of the phytochemicals in ZAE responsible for capping and stabilization of the Ag NPs. The FTIR spectrum exhibited major peaks at 3430, 2922, 2852, 1621, 1399 and 1049 cm^{-1} as shown in Fig. 1b. Among these, the peak at 3430 cm^{-1} corresponds to N–H stretching vibrations, indicates the presence of amine or amide groups. The peaks observed at 2922 cm^{-1} and 2852 cm^{-1} were due to the medium C-H stretching of the alkane. The peak at 3431 cm^{-1} is attributed to N-H stretching, while the band at 2922 cm^{-1} indicates aliphatic C–H stretching [35]. The peak appeared at 1621 cm^{-1}, implying the

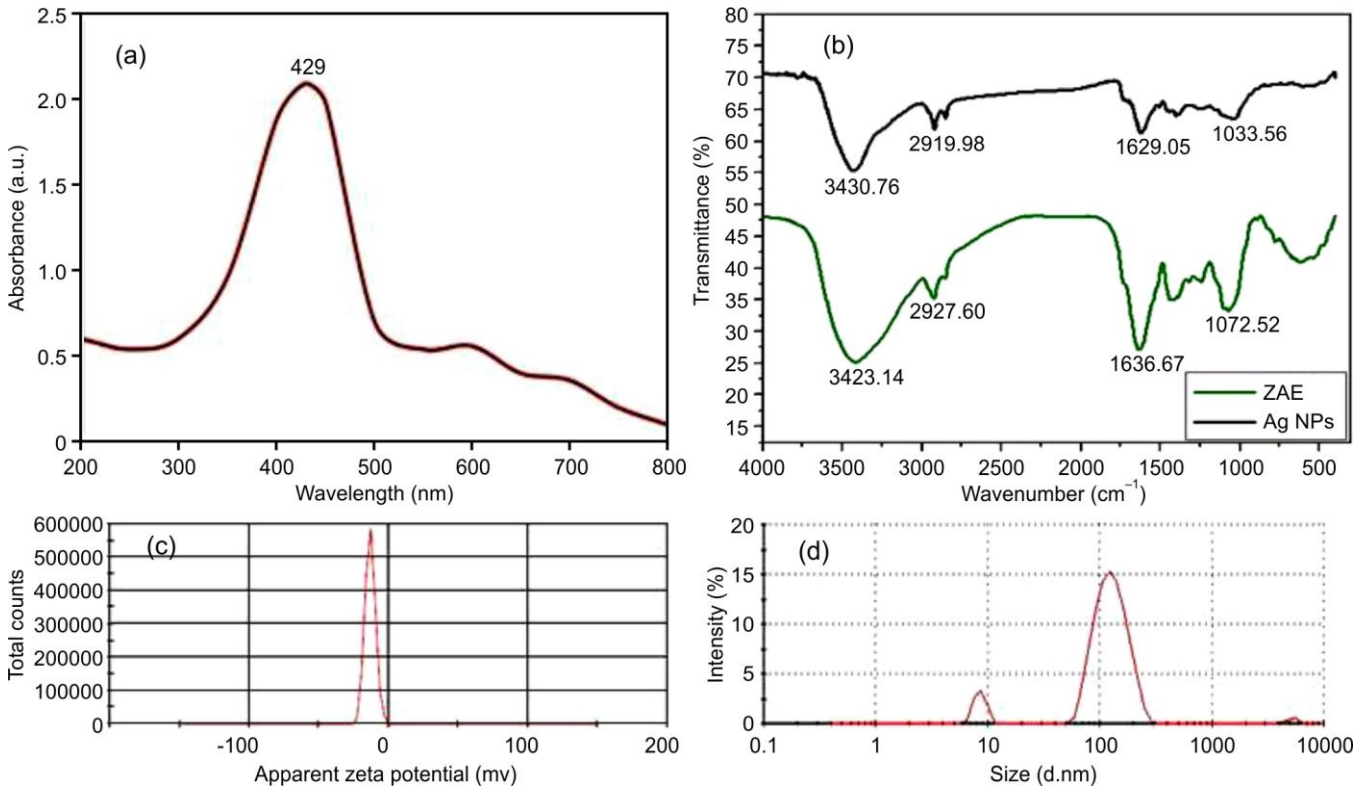

Fig. 1. Characterization of biosynthesized ZA-Ag NPs (a) UV-vis, (b) FTIR, (c) and (d) DLS

presence of secondary amines. The peaks at 1399 cm^{-1} and 1049 cm^{-1} were attributed to O-H bending of phenolic groups and strong, broad C-O-C stretching vibrations of anhydrides, respectively. Whereas, the peaks observed at 1378 cm^{-1} and 1044 cm^{-1} correspond to phenolic O-H bending and anhydride C-O-C stretching, respectively [36].

Dynamic light scattering (DLS) studies: DLS analysis revealed that Ag NPs had an average hydrodynamic diameter of 92 nm (Fig. 1c-d) and a PDI of 0.363, indicating a moderately monodisperse distribution. PDI values typically range from 0.05 to 0.7, with values closer to zero indicating higher monodispersity and values above 0.7 suggesting polydispersity [37]. The zeta potential of Ag NPs was -13.2 mV (Fig. 1c), implying good colloidal stability due to the sufficient electrostatic repulsion preventing particle aggregation. These findings are consistent with previous studies, which reported Ag NPs synthesized using *Urtica dioica* leaf extract with a PDI of 0.47 and a zeta potential of -15.5 mV [38].

SEM studies: The SEM image of ZA-Ag NPs (Fig. 2) shows that Ag NPs are predominantly spherical, appearing both as dispersed and in aggregated forms. These observations are consistent with the findings of Riaz *et al.* [39], observed similar characteristics in Ag NPs synthesized from *Z. armatum* bark extract with a few irregularly shaped particles. The observed aggregation is likely due to the adherence of phytochemical residues from the extract to the nanoparticle surfaces, as also reported by Zare-Bidaki *et al*. [40].

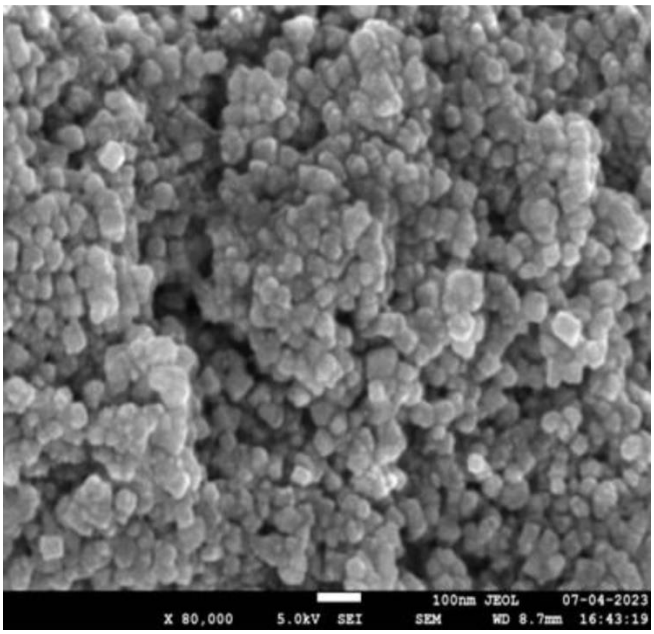

Fig. 2. SEM image of Ag NPs synthesized from the leaves extract of *Z. armatum*

X-ray diffraction: The broad diffraction peaks observed at angles 27.82º, 32.26º, 46.24º, 54.82º and 76.82º in the 2θ range confirm that the synthesized Ag NPs are composed of silver and exhibit crystalline characteristics (Fig. 3). The initial bulge observed in the XRD spectrum may be attributed to carbon incorporated into the nanoparticles from the plant extract. A comparable result was observed with silver nanoparticles synthesized using *Z. armatum* [35].

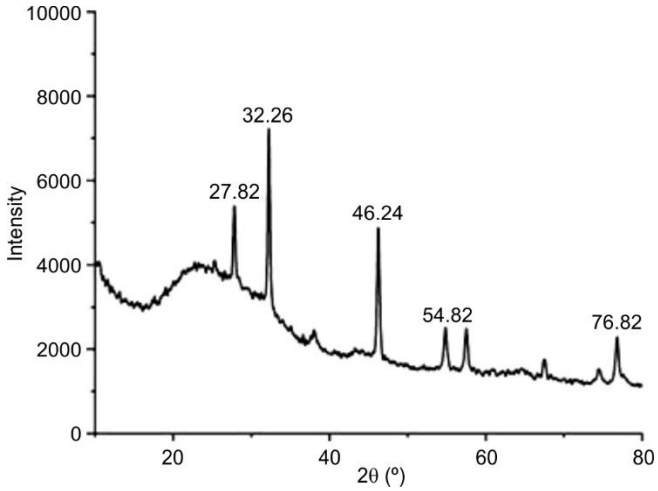

Fig. 3. XRD spectra of Ag NPs synthesized from the leaves extract of *Z. armatum*

***In vitro* cytotoxic activity:** Silver nanoparticles exert their cytotoxic effects primarily by inducing oxidative stress through generating reactive oxygen species [41]. The current findings (Fig. 4) revealed that Ag NPs at concentrations ranging from 0.02-16.6 µg/mL showed no significant effect on cell viability, whereas concentrations exceeding 50 µg/mL led to a marked reduction in viability. These findings are consistent with previously reported cytotoxic effects on Vero kidney cells [42]. In present study, the Ag NPs demonstrated a lethal concentration (LC_{50}) of 61.35 µg/mL, which represents the concentration that reduces the viability of 50% of the exposed cells. This LC_{50} value is slightly lower than those reported in previous studies, including 67.53 µg/mL and 66 µg/mL for Ag NPs tested against Vero and MDA-MB-231 cells, respectively [24,43].

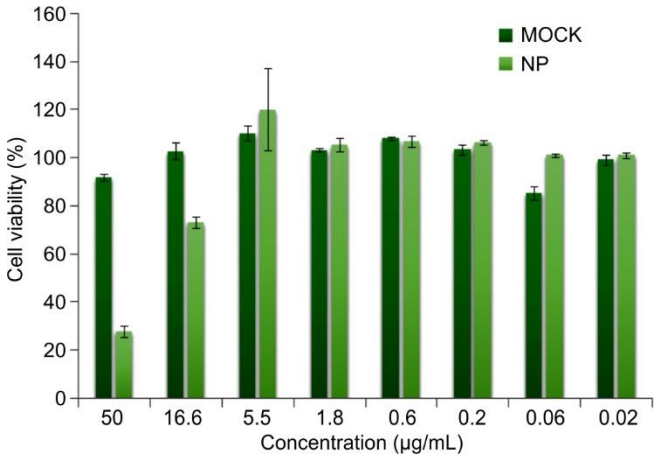

Fig. 4. Cytotoxicity assessment of Ag NPs synthesized from the leaves extract of *Z. armatum* on Vero kidney cells using MTT assay

Antidiabetic activity: The antidiabetic potential of ZA-Ag NPs and the plant extract (ZAE) was evaluated by assessing their inhibitory effects on α-amylase, α-glucosidase, β-glucosidase and lipase. The IC_{50} values of Ag NPs and ZAE required to inhibit these enzymes are mentioned in Table-1. These enzymes play key roles in carbohydrate digestion, breaking down oligosaccharides and disaccharides into absorb-

TABLE-1
IC_{50} VALUES OF ZAE, ZA-Ag NPs AND
STANDARD DRUG AGAINST DIFFERENT ENZYMES

Antidiabetic enzymes	IC_{50} (µg/mL)		
	ZAE	ZA-Ag NPs	Standard drug
α-Amylase	93.05	81.66	53.52
α-Glucosidase	77.56	61.79	36.30
β-Glucosidase	92.75	79.35	79.57
Lipase	18.84	39.18	02.46

able monosaccharides [44]. The suppression of these enzymes is notably effective for treating non-insulin-dependent diabetes, as it reduces the rate of glucose release into the blood [45].

α-Amylase assay: The Ag NPs exhibited stronger enzyme inhibition than the plant extract, although they were slightly less effective than the standard drug acarbose. In present study, Ag NPs exhibited inhibition rates of 11.47%, 17.53%, 32.68%, 48.48% and 65.15% at concentrations ranging from 20-100 µg/mL as indicated in Fig. 5a. The findings are in close agreement with those observed for *Fagonia cretica*-mediated Ag NPs at comparable concentrations [10]. The IC_{50} values were calculated as 77.52 µg/mL for Ag NPs and 81.82 µg/mL for the plant extract, while the positive control, acarbose, showed a lower IC_{50} of 68.69 µg/mL, indicating its higher inhibitory potency. The IC_{50} of ZA-Ag NPs was better than Ag NPs synthesized from aqueous leaf extract of *Muntingia calabura* [46]. Furthermore, the inhibitory activity of Ag NPs increased with concentration, significantly ($p < 0.05$) greater than that of the corresponding plant extract [47].

α-Glucosidase assay: The Ag NPs and crude plant extract effectively inhibited α-glucosidase in a dose-dependent manner (20-100 µg/mL) as shown in Fig. 5b, with the Ag NPs showing a greater reduction in enzymatic activity, consistent with the previously reported findings [48]. The results revealed that ZA-Ag NPs exhibit stronger α-glucosidase inhibitory activity than both the crude plant extract and Ag NPs derived from *Myristica fragrans* seeds [49]. The IC_{50} values of ZA-Ag NPs and ZAE against α-glucosidase were 75.72 and 82.77 µg/mL, respectively (Table-1), which aligns with the results reported for diethyl ether fractions of *Cornus capitate* [30]. Furthermore, the crude extract and Ag NPs of *Z. armatum* exhibited

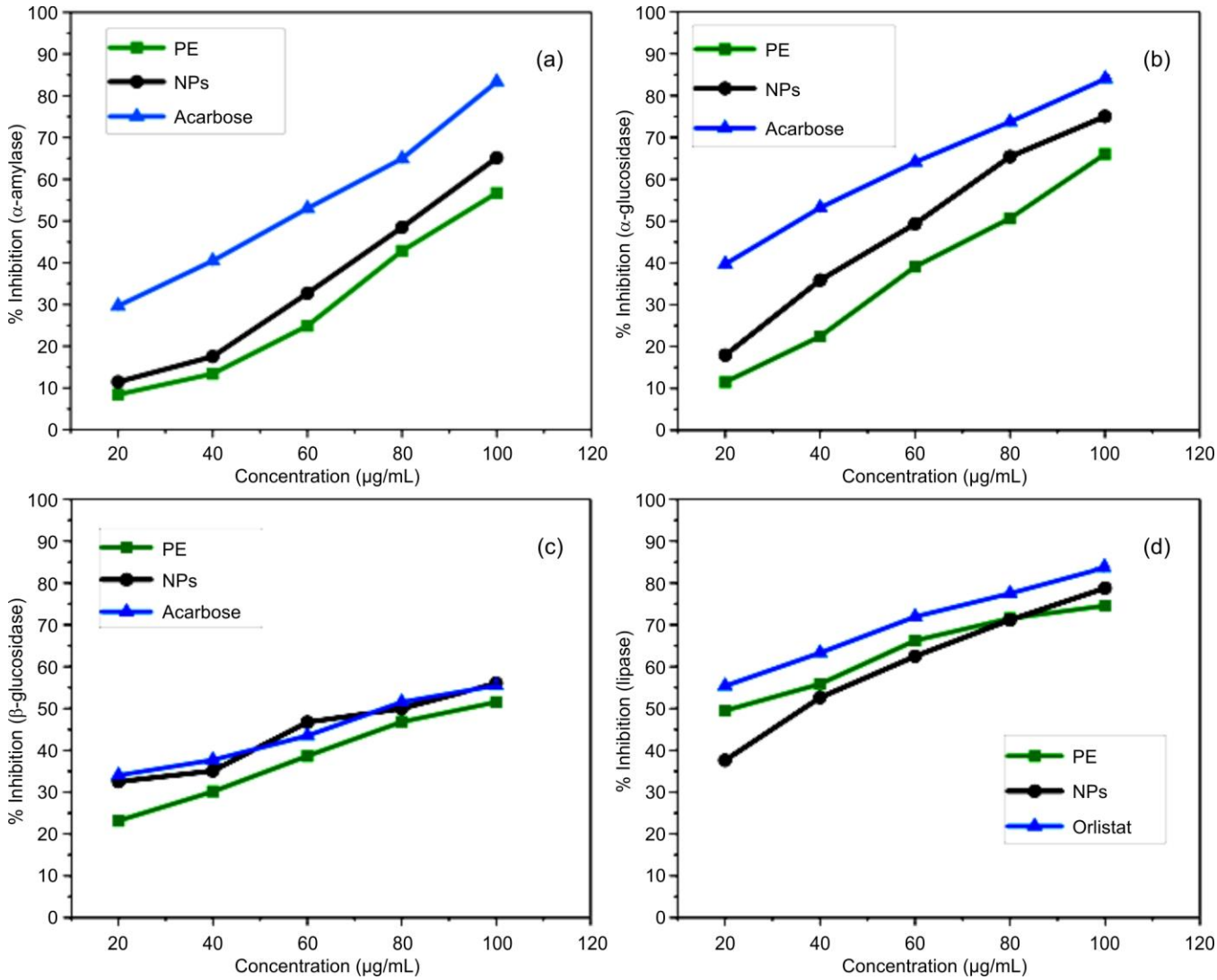

Fig. 5. Antidiabetic activity of ZA-Ag NPs, ZAE and standard drugs against (a) α-amylase, (b) α-glucosidase, (c) β-glucosidase and (d) lipase

significant ($p < 0.05$) α-glucosidase inhibitory activity that increased with concentration, corroborating the results of Jini and Sharmila (2020) [47].

β-Glucosidase assay: Both the Ag NPs and the plant extract ZAE demonstrated (Fig. 5c) concentration-dependent inhibition (20 to 100 µg/mL), with Ag NPs showing inhibition rates ranging from 32.50% to 56.03% and the plant extract from 23.18% to 51.52%. These results are consistent with those reported from the aqueous leaves extract of *Z. armatum* [19]. The Ag NPs exhibited promising inhibitory potential compared to acarbose, likely due to their enhanced ability to bind with β-glucosidase, thereby interfering with its enzymeatic activity and reducing the breakdown of complex carbohydrates into glucose [46]. The result revealed that Ag NPs showed stronger inhibitory effect than the plant extract and showed comparable activity to acarbose at concentrations of 20-100 µg/mL, consistent with the findings on *Morinda lucida* leaves extract [31]. The IC_{50} values for Ag NPs and plant extract were found to be 111.71 and 120.08 µg/mL, respectively, which are comparable to the orlistat IC_{50} of 114.78 µg/mL. The biosynthesized Ag NPs effectively regulate blood sugar by inhibiting β-glucosidase, making them promising candidates for antidiabetic treatments [49,50]. Statistical analysis revealed significant differences in β-glucosidase inhibition between ZAE and Ag NPs at all tested concentrations, showing concentration-dependent inhibition ($p < 0.01$), this demonstrates higher efficacy compared to the significance ($p < 0.05$) [50].

Lipase inhibition assay: Fig. 5d revealed that at concentrations of 20-100 µg/mL, Ag NPs inhibited lipase by 37.61% to 78.79%, while the plant extract showed inhibition ranging from 49.70% to 74.55%. The results were superior to those obtained with the ethanolic and aqueous extracts of *Heteromorpha arborescens* [32]. Although Ag NPs showed better inhibition than the plant extract, both were less effective than orlistat. It is the only approved long-term pancreatic lipase inhibitor for obesity [51]. The Ag NPs exhibited an IC_{50} value of 59.02 µg/mL. In comparison, the ZAE exhibited an IC_{50} of 49.24 µg/mL, demonstrating stronger lipase inhibitory activity than the ethyl acetate, dichloromethane and hexane leaves extracts. However, they were less effective than the aqueous and butanol fractions of *Bauhinia forficate* [52]. The lipase inhibition observed in this study was significant ($p < 0.05$) and comparable to the findings of Swierczewska *et al.* [53], who reported similar activity in fruit extracts of *Cornus mas* and *Cornus alba* [53].

Conclusion

This study assessed the antidiabetic potential of biologically synthesized silver nanoparticles (Ag NPs) and *Zanthoxylum armatum* extract (ZAE). The Ag NPs were produced using leaf extract from *Z. armatum* and characterized using UV-Vis spectrophotometry, which displayed a peak at 429 nm, indicating successful nanoparticle synthesis. FE-SEM confirmed that the biosynthesized Ag NPs possess a spherical morphology, while dynamic light scattering (DLS) analysis revealed an average particle size of 92.64 nm, with a polydispersity index (PDI) of 0.36 and a zeta potential of -13.2 mV, confirming their monodispersity and stability. The findings demonstrated that both ZAE and Ag NPs effectively inhibited α-amylase, α-glucosidase, β-glucosidase and lipase *in vitro*, with no observed toxicity to Vero cells. Consequently, they present a promising alternative for managing type 2 diabetes mellitus. However, additional *in vitro* and *in vivo* investigations are necessary to validate the safety and efficacy of ZA-Ag NPs as a treatment for diabetes with minimal side effects. This study provides a foundation for future research, particularly in the extraction, identification and characterization of the active secondary metabolites that contribute to the antidiabetic effects of ZAE and ZA-Ag NPs.

CONFLICT OF INTEREST

The authors declare that there is no conflict of interests regarding the publication of this article.

REFERENCES

1. S. Maiti, S. Akhtar, A.K. Upadhyay and S.K. Mohanty, *Sci. Rep.*, **13**, 2971 (2023); https://doi.org/10.1038/s41598-023-29978-y
2. N. Mantri, A.D. Goel, M. Patel, P. Baskaran, G. Dutta, M.K. Gupta, V. Yadav, M. Mittal, S. Shekhar and P. Bhardwaj, *BMC Public Health*, **24**, 527 (2024); https://doi.org/10.1186/s12889-024-18024-9
3. I.D.F. Diabetes Atlas, 2025 | Global Diabetes Data & Insights (2025); https://diabetesatlas.org/resources/idf-diabetes-atlas-2025/ (accessed June 4, 2025).
4. S. Jadoun, R. Arif, N.K. Jangid and R.K. Meena, *Environ. Chem. Lett.*, **19**, 355 (2021); https://doi.org/10.1007/s10311-020-01074-x
5. K.K. Verma, B. Kumar, H. Raj and A. Sharma, *J. Drug Deliv. Ther.*, **11(2-S)**, 136 (2021); https://doi.org/10.22270/jddt.v11i2-S.4786
6. S. Dewanjee, P. Chakraborty, B. Mukherjee and V. De Feo, *Int. J. Mol. Sci.*, **21**, 2217 (2020); https://doi.org/10.3390/ijms210622
7. A. Safipour Afshar and F. Saeid Nematpour, *Jentashapir J. Cell. Mol. Biol.*, **12**, 112437 (2021); https://doi.org/10.5812/jjcmb.112437
8. P. Kuppusamy, M.M. Yusoff, G.P. Maniam and N. Govindan, *Saudi Pharm. J.*, **24**, 473 (2016); https://doi.org/10.1016/j.jsps.2014.11.013
9. J. Dai and R.J. Mumper, *Molecules*, **15**, 7313 (2010); https://doi.org/10.3390/molecules15107313
10. M. Khan, M. Khan, S.F. Adil and H.Z. Alkhathlan, *Saudi J. Biol. Sci.*, **29**, 1801 (2022); https://doi.org/10.1016/j.sjbs.2021.10.045
11. M. Liu, R. Wang, M.P.M. Hoi, Y. Wang, S. Wang, G. Li, C.T. Vong and C.-M. Chong, *Int. J. Nanomedicine*, **20**, 6221 (2025); https://doi.org/10.2147/IJN.S508875
12. Ranjana, Z. Nooreen, U. Bushra, Jyotshna, D.U. Bawankule, K. Shanker, A. Ahmad and S. Tandon, *J. Ethnopharmacol.*, **230**, 1 (2019); https://doi.org/10.1016/j.jep.2018.10.018
13. T.P. Singh and O.M. Singh, *Indian J. Nat. Prod. Resour.*, **2**, 275 (2011).
14. C.P. Kala, N.A. Farooquee and U. Dhar, *Conserv. Soc.*, **3**, 224 (2005).
15. V. Bhatt, N. Kumar, U. Sharma and B. Singh, *Sep. Sci. Plus*, **1**, 311 (2018); https://doi.org/10.1002/sscp.201800004
16. S.N. Gilani, A.U. Khan and A.H. Gilani, *Phytother. Res.*, **24**, 553 (2010); https://doi.org/10.1002/ptr.2979
17. Z. Nooreen, S. Singh, D.K. Singh, S. Tandon, A. Ahmad and S. Luqman, *Biomed. Pharmacother.*, **89**, 366 (2017); https://doi.org/10.1016/j.biopha.2017.02.040
18. M.H. Khan and P.S. Yadava, *Indian J. Tradit. Knowl.*, **9**, 510 (2010).
19. C.V. Rynjah, N.N. Devi, N. Khongthaw, D. Syiem and S. Majaw, *J. Tradit. Complement. Med.*, **8**, 134 (2018); https://doi.org/10.1016/j.jtcme.2017.04.007

20. A. Dhami, A. Singh, D. Palariya, R. Kumar, O. Prakash, D.S. Rawat and A.K. Pant, *J. Essent. Oil-Bear. Plants*, **22**, 660 (2019); https://doi.org/10.1080/0972060X.2019.1630015
21. M.E. Shehata, G.M. El-Sherbiny, M.H. Sharaf, M.H. Kalaba and A.S. Shaban, *Biomass Convers. Biorefin.*, **15**, 3753 (2024); https://doi.org/10.1007/s13399-024-05301-1
22. A. Bhardwaj and N. Gupta, *Chem. Africa*, **8**, 1509 (2025); https://doi.org/10.1007/s42250-025-01192-5
23. S. Bawazeer, A. Rauf, S.U.A. Shah, A.M. Shawky, Y.S. Al-Awthan, O.S. Bahattab, G. Uddin, J. Sabir and M.A. El-Esawi, *Green Process. Synth.*, **10**, 85 (2021); https://doi.org/10.1515/gps-2021-0003
24. A.M. Sivalingam and A. Pandian, *Carbohydr. Polym. Technol. Appl.*, **8**, 100535 (2024); https://doi.org/10.1016/j.carpta.2024.100535
25. M. Khatun, Z. Khatun, M.R. Karim, M.R. Habib, M.H. Rahman and M.A. Aziz, *Food Chem. Adv.*, **3**, 100386 (2023); https://doi.org/10.1016/j.focha.2023.100386
26. N. Quadri, M.M. Setty, A. Awasthi, U. Nayak, M. Singh and S. Sharma, *Nanoscale*, **17**, 1555 (2025); https://doi.org/10.1039/D4NR03608E
27. S.N. Njeru and J.M. Muema, *BMC Res. Notes*, **14**, 57 (2021); https://doi.org/10.1186/s13104-021-05472-4
28. A.D. Afagnigni, M.A. Nyegue, S.V. Djova, F.X. Etoa and L.C.-M.S. Analysis, *J. Trop. Med.*, **2020**, 1 (2020); https://doi.org/10.1155/2020/5169847
29. S. Sekhon-Loodu and H.P.V. Rupasinghe, *Front. Nutr.*, **6**, 53 (2019); https://doi.org/10.3389/fnut.2019.00053
30. A. Bhatia, B. Singh, R. Arora and S. Arora, *BMC Complement. Altern. Med.*, **19**, 74 (2019); https://doi.org/10.1186/s12906-019-2482-z
31. M. Chokki, M. Cudalbeanu, C. Zongo, D. Dah-Nouvlessounon, I.O. Ghinea, B. Furdui, R. Raclea, A. Savadogo, L. Baba-Moussa, S.M. Avamescu, R.M. Dinica and F. Baba-Moussa, *Foods*, **9**, 434 (2020); https://doi.org/10.3390/foods9040434
32. T.O. Abifarin, G.A. Otunola and A.J. Afolayan, *Processes*, **9**, 1671 (2021); https://doi.org/10.3390/pr9091671
33. M. Naseer, U. Aslam, B. Khalid and B. Chen, *Sci. Rep.*, **10**, 9055 (2020); https://doi.org/10.1038/s41598-020-65949-3
34. N. Kaur, R. Kumar, S. Alhan, H. Sharma, N. Singh, R. Yogi, V. Chhokar, V. Beniwal, M. Kumar Ghosh, S. Kumar Chandraker, S. Rustagi and A. Kumar, *Inorg. Chem. Commun.*, **159**, 111735 (2024); https://doi.org/10.1016/j.inoche.2023.111735
35. K. Jyoti and A. Singh, *J. Genet. Eng. Biotechnol.*, **14**, 311 (2016); https://doi.org/10.1016/j.jgeb.2016.09.005
36. U. Habib, A. Ahmad Khan, T.U. Rahman, M.A. Zeb and W. Liaqat, *Microsc. Res. Tech.*, **85**, 3830 (2022); https://doi.org/10.1002/jemt.24231
37. I. Meydan, A. Aygun, R.N.E. Tiri, T. Gur, Y. Kocak, H. Seckin and F. Sen, *Environ. Sci. Adv.*, **3**, 28 (2024); https://doi.org/10.1039/D3VA00224A
38. M. Binsalah, S. Devanesan, M.S. Alsalhi, A. Nooh, O. Alghamdi and N. Nooh, *Microorganisms*, **10**, 789 (2022); https://doi.org/10.3390/microorganisms10040789
39. M. Riaz, M. Altaf, P. Ahmad, M.U. Khandaker, H. Osman, E.M. Eed and Y. Shakir, *Molecules*, **27**, 1166 (2022); https://doi.org/10.3390/molecules27041166
40. M. Zare-Bidaki, H. Aramjoo, Z.M. Mizwari, P. Mohammadparast-Tabas, R. Javanshir and S. Mortazavi-Derazkola, *Arab. J. Chem.*, **15**, 103842 (2022); https://doi.org/10.1016/j.arabjc.2022.103842
41. M.H. Sangour, I.M. Ali, Z.W. Atwan and A.A.A.L.A. Al Ali, *Egypt. J. Med. Hum. Genet.*, **22**, 9 (2021); https://doi.org/10.1186/s43042-020-00120-1
42. A.F. Shater, F.M. Saleh, Z.M. Mohammedsaleh, H. Gattan, B.M. Al-Ahmadi, N.H. Saeedi, M.M. Jalal and C. Panneerselvam, *Green Process. Synth.*, **12**, 20228111 (2023); https://doi.org/10.1515/gps-2022-8111
43. L. Ebrahimi, S. Hosseinzadeh, M. Pourmontaseri and J. Jalaei, *Sci. Surveill. Syst.*, **6**, 190 (2018).
44. K. Balan, W. Qing, Y. Wang, X. Liu, T. Palvannan, Y. Wang, F. Ma and Y. Zhang, *RSC Adv.*, **6**, 40162 (2016); https://doi.org/10.1039/C5RA24391B
45. A. Podsędek, I. Majewska, M. Redzynia, D. Sosnowska and M. Koziołkiewicz, *J. Agric. Food Chem.*, **62**, 4610 (2014); https://doi.org/10.1021/jf5008264
46. S. Vankudoth, S.B. Dharavath, P. Chirumamilla and S. Taduri, *Proc. Natl. Acad. Sci., India, Sect. B Biol. Sci.*, **94**, 1073 (2024); https://doi.org/10.1007/s40011-024-01650-z
47. D. Jini and S. Sharmila, *Mater. Today Proc.*, **22**, 432 (2020); https://doi.org/10.1016/j.matpr.2019.07.672
48. S. Majeed, M. Danish, N.A. Zakariya, R. Hashim, M.T. Ansari, S. Alkahtani and M.S. Hasnain, *Oxid. Med. Cell. Longev.*, **2022**, 1646687 (2022); https://doi.org/10.1155/2022/1646687
49. R. Perumalsamy and L. Krishnadhas, *Appl. Biochem. Biotechnol.*, **194**, 1136 (2022); https://doi.org/10.1007/s12010-022-03825-8
50. M.E. Gondokesumo, H.S.W. Kusuma and W. Widowati, *Cell. Biomed. Sci.*, **1**, 34 (2017); https://doi.org/10.21705/mcbs.v1i1.3
51. Y. Vangoori, A. Dakshinamoorthi and S. Kavimani, *Maedica*, **14**, 254 (2019); https://doi.org/10.26574/maedica.2019.14.3.254
52. R.R. Franco, V.H. Mota Alves, L.F. Ribeiro Zabisky, A.B. Justino, M.M. Martins, A.L. Saraiva, L.R. Goulart and F.S. Espindola, *Biomed. Pharmacother.*, **123**, 109798 (2020); https://doi.org/10.1016/j.biopha.2019.109798
53. A. Świerczewska, T. Buchholz, M.F. Melzig and M.E. Czerwińska, *J. Food Drug Anal.*, **27**, 249 (2019); https://doi.org/10.1016/j.jfda.2018.06.005